Charge disproportionation and spin ordering tendencies in Na$_x$CoO$_2$

K.-W. Lee,[1] J. Kuneš,[1,2] and W. E. Pickett[1]

[1]*Department of Physics, University of California, Davis, California 95616, USA*
[2]*Institute of Physics, Academy of Sciences, Cukrovarnická 10, CZ-162 53 Prague, Czech Republic*
(Received 23 February 2004; published 14 July 2004)

The strength and effect of Coulomb correlations in the (superconducting when hydrated) $x \approx 1/3$ and "enhanced" $x \approx 2/3$ regimes of Na$_x$CoO$_2$ are evaluated using the correlated band theory LDA+U (local density approximation of Hubbard U) method. Our results, neglecting quantum fluctuations, are (1) allowing only ferromagnetic order, there is a critical $U_c = 3$ eV, above which charge disproportionation occurs for both $x = 1/3$ and $x = 2/3$, (2) allowing antiferromagnetic order at $x = 1/3$, U_c drops to 1 eV for disproportionation, (3) disproportionation and gap opening occur simultaneously, and (4) in a Co^{3+}-Co^{4+} ordered state, antiferromagnetic coupling is favored over ferromagnetic, while below U_c ferromagnetism is favored. A comparison of the calculated Fermi level density of states compared to reported linear specific heat coefficients indicates enhancement of the order of five for $x \sim 0.7$, but negligible enhancement for $x \sim 0.3$. This trend is consistent with strong magnetic behavior and local moments (Curie-Weiss susceptibility) for $x > 0.5$ while there is no magnetic behavior or local moments reported for $x < 0.5$. We suggest that the phase diagram is characterized by a crossover from effective single-band character with $U \gg W$ for $x > 0.5$ into a three-band regime for $x < 0.5$, where $U \to U_{\text{eff}} \lesssim U/\sqrt{3} \sim W$ and correlation effects are substantially reduced.

PACS number(s): 75.25.+z, 71.28.+d, 71.27.+a

I. BACKGROUND

Since the discovery of high temperature superconductivity in cuprates, there has been intense interest in transition metal oxides with strongly layered (quasi) two-dimensional (2D) crystal structures and electronic properties. For a few years now alkali-metal intercalated layered cobaltates, particularly Na$_x$CoO$_2$ (NxCO) with $x \sim 0.50-0.75$, have been pursued for their thermoelectric properties.[1] The recent discovery[2] and confirmation[3–11] of superconductivity in the system Na$_x$CoO$_2 \cdot y$H$_2$O for $x \approx 0.3$ when intercalated with water at the $y \approx 0.3$ level, has heightened interest in the NxCO system. The structure[12–14] is based on a 2D CoO$_2$ layer in which edge-sharing CoO$_6$ octahedra lead to a triangular lattice of Co ions. Na donates its electron to the CoO$_2$ layer, hence x controls the doping level of the layer: $x=0$ corresponds to Co^{4+}, $S = \frac{1}{2}$ low spin ions with one minority t_{2g} hole, and $x = 1$ corresponds to nonmagnetic Co^{3+}.

Nearly all reports of nonstoichiometric materials quote values of x in the 0.3–0.8 range, and the materials generally seem to show metallic conductivity. The $x=1$ endpoint member NaCoO$_2$, with rhombohedral R$\bar{3}$m space group[15,16] is reported to be a conventional semiconductor.[17,18] The isovalent compound LiCoO$_2$ has been more thoroughly studied, with the conclusion that it is a nonmagnetic band insulator with 2.7 eV band gap.[19,20] The $x=0$ endpoint has been anticipated by many to be a t_{2g}^5 Mott insulator but is less studied; in fact, the Co^{4+} formal oxidation state in a stoichiometric compound is rare. The sulfur counterpart CoS$_2$ is metallic itinerant ferromagnet, close to being half metallic. A decade ago, Amatucci *et al.*[21] and Seguin *et al.*[22] reported synthesis of CoO$_2$ but were unable to identify a complete structure. They concluded initially that the Co ions lay on a *distorted* triangular lattice. More recently, a further study by Tarascon *et al.*[23] has traced the difficulty in pinning down the structure to the existence of two phases of CoO$_2$, one stoichiometric and the other having 4% oxygen vacancies. CoO$_2$ samples are metallic and nonmagnetic, hence they cannot be said to contain Co^{4+} ions.[24]

Much has been made of the similarities and differences of this cobaltate system compared to the cuprates. Both are layered transition metal oxide materials whose conductivity is strongly anisotropic. Both are in the vicinity of a Mott insulator (although the cobaltate one — CoO$_2$ — is not well characterized). It is possible to vary the carrier concentration (x in the cobaltate formula) in both systems, with the range in the cobaltates yet to be agreed on. In both systems there are specific superconducting regions: in the cuprates it is a "dome" $0.06 \leq x \leq 0.22$, roughly, while in the cobaltates there are reports both of a dome $0.27 \leq x \leq 0.33$ (Ref. 11) and of a $T_c = 4.5$ K plateau for $0.28 \leq x \leq 0.37$.[25] However, the differences between the cobaltates and cuprates are substantial and expected to be crucial. Cobalt forms a triangular lattice, which frustrates antiferromagnetic (AFM) order, while the bipartite square Cu lattice invites AFM order. The CoO$_6$ octahedra are edge-sharing, rather than corner-sharing, making the bandwidth much narrower and the exchange coupling smaller. The cobaltates are electron-doped from the (anticipated) Mott insulator, as opposed to the most common hole-doped cuprates. Most striking, possibly: In the cobaltates $T_c^{\text{max}} = 4.5$ K compared to $T_c^{\text{max}} = 130$ K (or higher under pressure) in cuprates.

Another system for comparison is the transition metal disulfide based one, with Na$_{1/3}$TaS$_2 \cdot y$H$_2$O as the primary comparison. In the (Nb, Ta)(S, Se)$_2$ system, charge-density waves compete with superconducting pairing for the Fermi surface, with coexistence occurring in certain cases. The structure of the (for example) TaS$_2$ layer is identical to that of the CoO$_2$ layer, consisting of edge-sharing transition metal chalcogenide octahedrons. In these dichalcogenides, as in

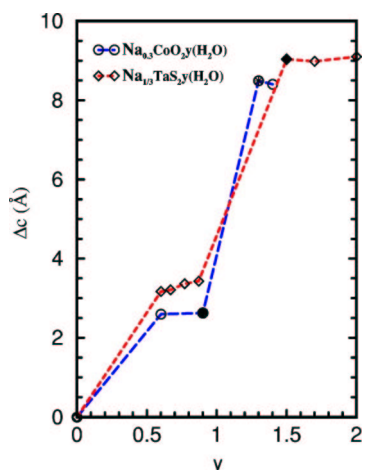FIG. 1. Change in the c axis lattice parameter with the addition of H_2O, in the two systems $Na_{0.3}CoO_2 \cdot H_2O$ and $Na_{1/3}TaS_2 \cdot H_2O$, illustrating the great similarity. For cobaltates, data are from Foo *et al.* (Ref. 33) (empty circles), Jin *et al.* (Ref. 9) (filled circle), and Schaak *et al.* (Ref. 11) (asterisk). For the chalcogenides, data are from Johnston (Ref. 29) (empty diamonds) and Johnston and Frysinger (Ref. 30) (filled diamonds).

the cobaltate system, two well-defined stages of hydration have been identified.[26] In the first stage H_2O is incorporated into the same layer as the cation (typically an alkali ion), and in the second stage two H_2O layers are formed on either side of the cation layer. The similarity in increase in the c lattice parameter compared to the cobaltates is illustrated in Fig. 1.

The electron concentration in $Na_{1/3}TaS_2 \cdot yH_2O$ is specified by the Na concentration $x=1/3$, and in this system superconductivity occurs at 4–5 K (the same range as in the cobaltates) *regardless* of the concentration y of water molecules intercalated into the structure.[27] Specific thermodynamically stable phases were identified at $y=0, 2/3, 0.8, 1.5,$ and 2.[28–30] The level of electron donation seems to be crucial: using $Y_{1/9}$ and $La_{1/9}$ based on the trivalent ions leads to the same superconducting transition temperature. Using the divalent ion Mn ($d^5, S=5/2$), at the same electron donation level $Mn_{1/6}TaS_2$ is *ferromagnetic* (FM). Intercalating this FM compound with H_2O leads again to $T_c \sim 4$ K. This latter behavior is understood as the water-induced separation of TaS_2 layers decreasing the interlayer magnetic coupling sufficiently to inhibit long-range magnetic order, thereby allowing the innate superconducting tendency in the doped TaS_2 layer to assert itself.

Much of the emphasis, both experimental and theoretical, has been directed toward the superconducting behavior of the cobaltates, but the long-known behavior of the tantalum disulfides just mentioned suggests the superconductivity may not be so distinctive. Reports of the magnetic behavior in these cobaltates have been of particular interest to us. Except for a charge disproportionated and charge-ordered phase in a narrow range around $x=0.5$ (Ref. 31) identified by its insulating behavior, all samples are reported to be metallic. For x in the 0.5–0.8 range, the susceptibility $\chi(T)$ is Curie-Weiss-like with reported moment of order 1 μ_B per Co^{4+}.[2,3,9] This local moment is normally interpreted as indicating the presence of correlated electron behavior on the Co sublattice, and

most theoretical treatments have assumed this viewpoint.

Some phase transitions have been reported in the high x region. Magnetic ordering at 22 K with small ordered moment has been reported for $x=0.75$ (Ref. 33) based on transport and thermodynamic data, and the same conclusion was reached by Sugiyama *et al.* from μSR studies.[34,35] Boothroyd *et al.* performed inelastic neutron scattering on $x=0.75$ single crystals and observed FM spin fluctuations.[36] Field dependence of the thermopower measured by Wang *et al.*[10] indicated that the spin entropy of the magnetic Co system (i.e., the spins of the Co^{4+} ions) is responsible for the unusual thermoelectric behavior. For $x=0.55$, Ando *et al.* reported[37] a rather large linear specific heat coefficient $\gamma = 56$ mJ/mol K^3. Thus for $x > 0.5$ magnetic Co ions are evident and are strongly influencing the electronic low energy excitations.

However, for samples with $x \approx 0.3$ (i.e., the superconducting phase) many reports concur that the Curie-Weiss behavior of χ vanishes.[3,8,9,38,39] In addition, the specific heat γ is much smaller, with values around 12 mJ/mol K^2 reported.[4,5] It is extremely curious that local moments should vanish so near to what has been believed would correspond to a Mott insulator ($x=0$, Co^{4+} in CoO_2), and that superconductivity appears only in the moment-free regime. In the strongly interacting single-band triangular lattice picture, the $x=0$ system corresponds to the half-filled triangular lattice that has been studied extensively for local singlet (resonating valence bond) behavior.[40] The ground state of that model has however been found to be Néel ordered.[41] In any case, the $x \approx 0.3$ region of superconductivity in NxCO is however well away from the expected Mott-insulating regime, and the behavior in such systems is expected to vary strongly with doping level.

Much of the language used in characterizing this system (above, and elsewhere) has been based on the local orbital, single-band picture. As discussed more fully below, the doping in this system occurs within the threefold t_{2g} complex of the Co ion, with degeneracy only slightly lifted by the noncubic structure. The question of single-band versus multiband nature of this cobaltate system is possibly one of the more important issues to address, because it can strongly affect the tendency toward correlated electron behavior.

Although the primary interest has been in the superconductivity of NxCO, there is first a real need to understand the electronic structure of the normal state of the unhydrated material, and its dependence on the doping level x. The electronic structure of the $x=1/2$ (with ordered Na) compound in the local density approximation (LDA) has been described by Singh.[42,43] Within LDA all Co ions are identical ("$Co^{3.5+}$"), the Co t_{2g} states are crystal-field split (by 2.5 eV) from the e_g states, and the t_{2g} bands are partially filled, consequently the system is metallic consistent with the observed conductivity. The t_{2g} band complex is $W \approx 1.5$ eV wide, and is separated from the 5 eV wide O $2p$ bands that lie just below the Co d bands. Singh suggested that the expected on-site Coulomb repulsion (which has not been calculated) is $U=5-8$ eV on Co, which gives $U \gg W$ so that correlation effects can be anticipated.

Notwithstanding the experimental evidence for nonmagnetic Co ions in the superconducting material, most of the

theoretical discussion[44–51] has focused on the strongly inter-acting limit, where U is not only important, but in fact is presumed to be so large that it prohibits double occupancy, as described by the single band t-J model. The lack of local moments and only weak to moderate enhancement of the specific heat γ suggests that a more realistic picture may be required. Undoubtedly the single band scenario is a limited one: Although the rhombohedral symmetry of the Co site splits the t_{2g} states into a_g and e'_g representations, the near-octahedral symmetry makes them quasidegenerate. Koshibae and Maekawa have shown that the band dispersion in the t_{2g} band complex in these cobaltates displays unexpected intri-cacies, including some analogies to a Kagomé lattice.[52]

In this paper we begin to address the correlation question by taking the strongly correlated viewpoint and using the correlated band theory LDA+Hubbard U (LDA+U) method. We investigate two distinct regions of the phase dia-gram by focusing on $x=1/3$, the regime where superconduc-tivity emerges, and $x=2/3$ where more magnetic behavior is observed. We find that $U \gtrsim U_c = 3$ eV leads to charge dispro-portionation (CD) and gap opening for both $x=1/3$ and $x=2/3$ if only FM order is allowed. For the Néel ordered case at $x=1/3$, the corresponding transition occurs at $U_c = 1$ eV. The availability of three distinct sublattices for the ordering, coupled with strong 2D fluctuations, may destroy long-range order and make local probes important in studying charge disproportionation and correlation. The small values of U_c that we obtain even for $x=1/3$ tend to confuse the theoretical picture, since there seems to be a conspicuous absence of correlated electron behavior in this regime of doping.

II. STRUCTURE AND METHOD OF CALCULATION

Our calculations are based on the hexagonal structure (space group $P6_322$), obtained by Jansen and Hoppe, having lattice constants ($a=2.84$ Å, $c=10.81$ Å).[53] The supercell ($\sqrt{3}a \times \sqrt{3}a \times c/2$) is used so that at the concentration $x=1/3$ that we consider, two (or possibly three) inequivalent Co ions, viz. Co^{3+} and Co^{4+}, are allowed to emerge in the process of self-consistency. The allowed order is displayed in Fig. 2. Since we are not analyzing the very small interlayer coupling here, a single layer cell is used. In the supercell (space-group $P\bar{3}1m$, No. 157), atomic coordinations are Na at the $1a$ $(0,0,1/2)$ above/below the Co site at the $1a$ $(0,0,0)$, and the other Co sites are the $2b$ $(1/3,2/3,0)$. Oxy-gen sites are the $3c$ $(2/3,0,\bar{z}_0)$ and the $3c$ $(1/3, 0, z_0)$ posi-tions, respectively. The O height $z_0 = 0.168(c/2) = 0.908$ Å, which is relaxed by LDA calculation,[42] produces the Co-O-Co bond angle 98.5° (90° for undistorted), so that the octahedra are considerably distorted.

Two all-electron full-potential electronic methods have been used. The full-potential linearized augmented-plane-waves (FLAPW) as implemented in WIEN2K code (Ref. 54) and its LDA+U (Refs. 55 and 56) extension were used. The s,p, and d states were treated using the augmented plane wave+local orbitals (APW+lo) scheme,[57] while the stan-dard LAPW expansion was used for higher l's. Local orbitals were added to describe Co $3d$ and O $2s$ and $2p$ states. The basis size was determined by $R_{mt}K_{max} = 7.0$. The full-
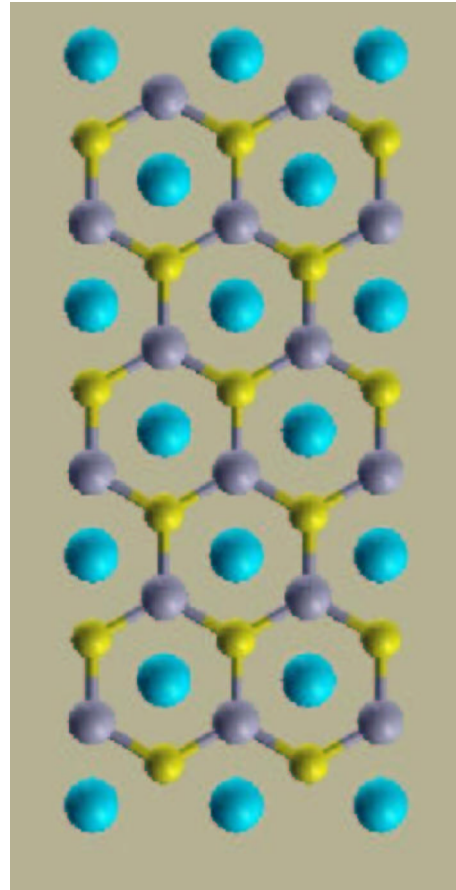

FIG. 2. Illustration of the type of charge disproportionation and spin ordering that is allowed in the chosen $\sqrt{3} \times \sqrt{3}$ supercell. The unconnected large spheres represent nonmagnetic Co^{3+} ions, while the large and small connected spheres represent oppositely directed Co^{4+} spins when ordered antiferromagnetically.

potential nonorthogonal local-orbital minimum-basis scheme (FPLO) (Refs. 58 and 59) was also used. Valence orbitals included Na $2s2p3s3p3d$, Co $3s3p4s4p3d$, and O $2s2p3s3p3d$. The Brillouin zone was sampled with regular mesh containing 50 irreducible k-points. Both popular forms[60,61] of the LDA+U functional have been used in our calculations, with no important differences being noticed.

III. WEAKLY CORRELATED LIMIT

LDA electronic structure at $x=1/3$. The e_g-t_{2g} crystal field splitting of 2.5 eV that can be seen in the full band plot in Fig. 3 places the (unoccupied) e_g states (1 eV wide) well out of consideration for most low energy effects. The O $2p$ band complex begins just below the bottom of the t_{2g} bands (see Fig. 3) and is 5.5 eV wide. The states into which holes are doped from $NaCoO_2$ come from the 1.6 eV wide t_{2g} band complex. The trigonal symmetry of the Co site in this trian-gular CoO_2 layer splits the t_{2g} states into one of a_g symmetry $[(|xy\rangle+|yz\rangle+|zx\rangle)/\sqrt{3}$ in the local CoO_6 octahedron coordi-nate system] and a doubly degenerate pair e'_g $[(|xy\rangle+\alpha|yz\rangle+\alpha^2|zx\rangle)\sqrt{3}$ and its complex conjugate, where $\alpha = \exp(2\pi i/3)]$.

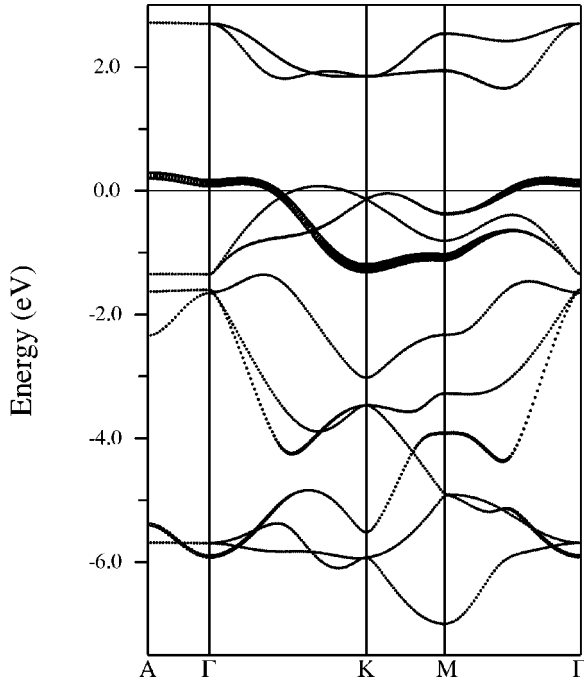FIG. 3. Local density approximation bands of $Na_{1/3}CoO_2$ in the virtual crystal approximation where there is one Co ion per cell, shown along the principal high symmetry directions. The e_g bands lie above 1.5 eV; the bands below −1.5 eV are predominantly oxygen $2p$ in character. The thickened lines emphasize the bands within the t_{2g} complex (−1.5 to 0.5 eV) with strong a_g character.

The t_{2g} band complex that is intersected by the Fermi level E_F is shown in more detail in Fig. 4, where the bands with primarily a_g character are shown in the "fatbands" representation against the corresponding densities of states. The band dispersions agree well with those calculated by Rosner et al.[62] The a_g character is strong at the bottom of the t_{2g} complex as well as at the top, and illustrates that holes doped into the band-insulating $NaCoO_2$ ($x=1$) phase go initially
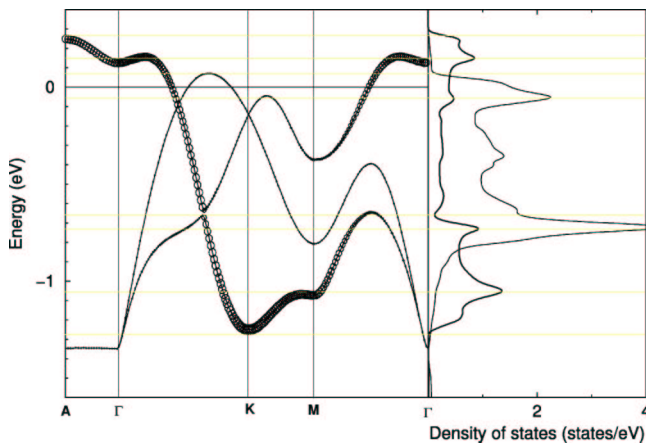

FIG. 4. Band structure (in the virtual crystal approximation) along high symmetry lines (left panel) and the aligned density of states (right panel) for the $x=1/3$ cobaltate in the local density approximation. The a_g symmetry band is emphasized with circles proportional to the amount of a_g character. The a_g density of states is indicated by the darker line.

into one a_g band that is rather flat for ∼25–30% of the distance to the zone boundary. Based on a rigid band interpretation using this $x=1/3$ density of states (DOS), doped holes enter only a_g states until $x≈0.6$, whereupon an e'_g Fermi surface begins to form. This observation is consistent with the $x=0.5$ Fermi surface shown by Singh[42] which has six e'_g cylinders.

It is of interest to view this band structure from the viewpoint of a single isolated tight-binding s-band on a triangular lattice with near-neighbor hopping only, which is intended[44–48,50] to model the a_g band dispersion. The a_g DOS lies higher than that of e'_g not because its band center lies higher (in fact its centroid is somewhat lower) but rather due to the particular dispersion and to a substantially larger effective bandwidth. Judged from the dispersion curves themselves, the a_g and e'_g bands differ little in width. However, nearly all of the e'_g states lie within a 1.0 eV region, whereas the a_g DOS extends over 1.5 eV.

The a_g band dispersion in Fig. 4 does resemble that of the simple tight-binding model $-t\Sigma_{\langle ij\rangle}(c_i^\dagger c_j+\text{H.c.})$ with a negative value of t. (The band structure also indicates that the e'_g hopping integral has the opposite sign to that of a_g.) The a_g-projected DOS however is nothing like that of the tight-binding model.[46] The reason is twofold. First, there is mixing of the a_g with the e'_g bands over most of the Brillouin zone. The hybridization is evident along the M-Γ line in Fig. 4; it is less obvious along the Γ-K line because the mixing happens to be accidentally small for the $x=1/3$ CoO_2 layer structure. For other Co-O distances and bond angles, and for $x=0$ doping level (not shown), the mixing of the a_g band with the lower e'_g band becomes much larger. A second reason for the actual shape of the DOS is due to the influence of some second-neighbor hopping,[62] which makes the a_g band near $k=0$ much flatter than the tight-binding model, or even disperse slightly upward before turning downward.

Some details of the band structure should be clarified. The upward dispersion of the a_g band around the Γ point (mentioned above) also seems to be affected by interlayer coupling, which can depress the band at $k=0$. Johannes and Singh have reported that, even for well separated CoO_2 layers (i.e., when hydrated) the a_g band may still disperse upward[63] before turning down. Even for CoO_2 layer geometries for which there is no upward curvature, the a_g band remains unusually flat out to almost 1/3 of the way to the zone boundary. Either behavior is indicative of extended hopping processes.

Magnetic order with LDA. Analogous to the results of Singh for $x=0.3,0.5,0.7$,[42,43] we find ferromagnetic (FM) tendencies for $x=1/3$ within LDA. In disagreement with experiment (no magnetic order is observed for $x≈0.3$, nor even any local moment at high temperature) a half metallic FM result is found, with a moment of 2 μ_B/supercell that is distributed almost evenly on the three Co ions. The exchange splitting of the t_{2g} states is 0.5 eV, and the Fermi level (E_F) lies just above the top of the fully occupied majority bands (the minority bands are metallic). The FM energy gain is about 45 meV/Co. With the majority bands filled, the filling of the minority t_{2g} bands becomes 2/3, leading to larger e'_g hole occupation than for the paramagnetic phase. Hence, un-
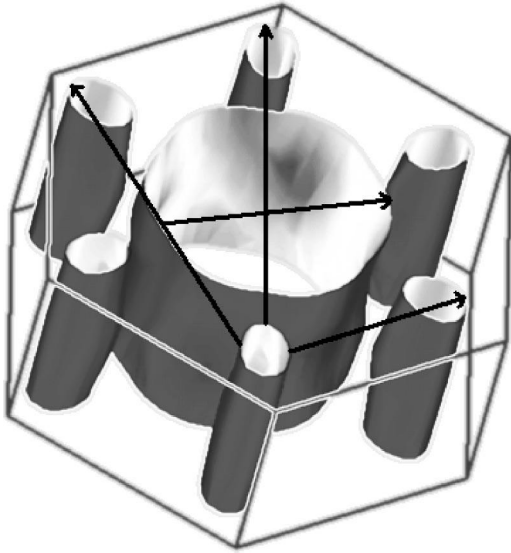
FIG. 5. Fermi surface for (virtual crystal) NxCO, $x=0.30$, in the two-dimensional Brillouin zone. The large cylinder contains a_g holes, whereas the six small cylinders contain holes that are primarily e'_g-like.

like the standard assumption being made so far, $x=1/3$ is a multiband ($a_g+e'_g$) system (within LDA, whether ferromagnetic or paramagnetic). Attempts using LDA to obtain self-consistent charge disproportionated states, or AFM spin ordering, always converged to the FM or nonmagnetic solution.

Fermiology. Suspecting from the $S=1/2$ spins and the two-dimensionality that quantum fluctuation is an important aspect of this system, it is possible that the $x=1/3$ system is a "fluctuation-induced paramagnet" due to the lack of account of fluctuations in the electronic structure calculations. Whatever the underlying reason, a page can be taken from the high T_c cuprate chapter of materials physics that, even in the presence of considerable correlation effects, in the magnetically disordered metallic phase the paramagnetic Fermi surface (FS) will emerge. The lack of any observed magnetic

behavior in the $x\approx0.3$ region reinforces this expectation.

In Fig. 5 we show the $x=1/3$ LDA FS, which is similar to the $x=0.5$ one shown by Singh.[43] A large Γ-centered hole cylinder (mean radius K_F) shows some flattening perpendicular to the $\Gamma-K$ direction, this cylinder holds $0.43a_g$ holes/Co. In addition, there are six additional, primarily e^f_g in character, hole cylinders lying along the Γ-K directions, containing 0.04 holes in each of the six small cylinders (radius k_F). The total is the 0.67 holes necessary to account for the $x=0.33$ electron count. This FS geometry leads to several important phase space features. There are the nesting wave vectors that translate one of the small cylinders into another, giving three distinct intercylinder nesting vectors as illustrated in Fig. 5. If these cylinders were circular, these vectors would represent strong nesting vectors for charge- or spin-density waves. In addition, the susceptibility for $Q \leq 2k_F$ intrasurface scattering processes is constant in two dimensions.[67] The calculated cylinders have an eccentricity of 1.25, weakening these nesting features somewhat. There are in addition the corresponding processes with $Q \leq 2K_F$ of the large cylinder.

IV. INCLUSION OF CORRELATION EFFECTS

Despite the feature of the LDA+U method that it drives local orbital occupations to integral occupancy (as U increases), to our knowledge it has never been used to study the question of charge disproportionation. In this section we show that moderate values of U lead to CD at both $x=1/3$ and $x=2/3$. For the triangular lattice, threefold expanded supercells ($\sqrt{3}\times\sqrt{3}$, see Sec. II) are convenient, and $x=1/3$ lies very close to the superconducting composition while $x=2/3$ is representative of the $x>0.5$ region that shows correlated behavior.[64]

LDA+U magnetic structure and energies. The behavior of the LDA+U results (Co moments and the energy gap) versus U was first studied for $x=1/3$ (on-site exchange was kept fixed at the conventional value of 1 eV as U was varied). The dependence of the magnetic moment and band gap on U for FM ordering is shown in the left panel of Fig. 6. For
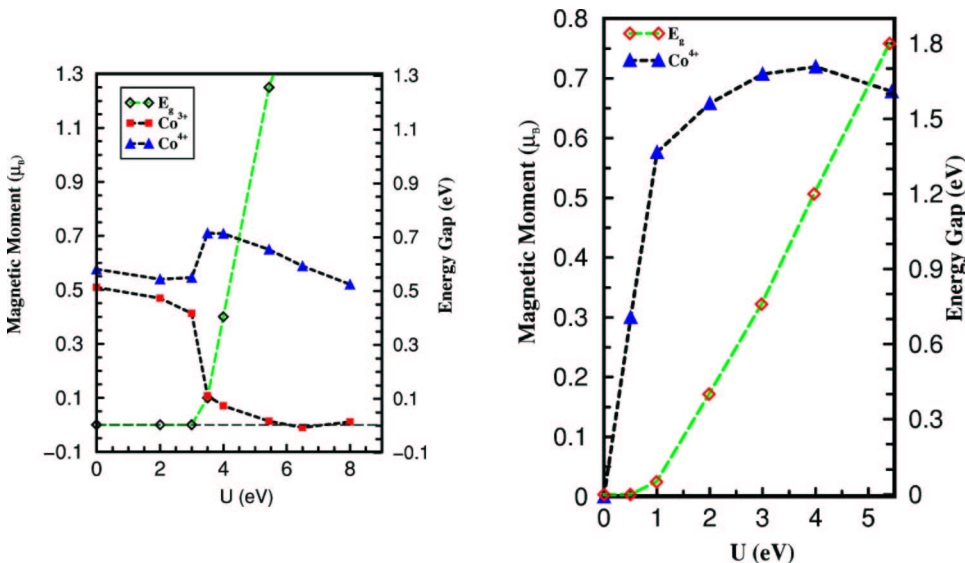

FIG. 6. Effect of the intra-atomic repulsion U on the magnetic moment (left axis) and energy gap (right axis) of the Co1 and Co2 ions in the supercell. Left panel: result for ferromagnetic order. Changes in the magnetic moments, indicating disproportionation to formal charge states Co^{3+} and Co^{4+}, begins at $U_c=3$ eV. The opening of the gap (half metallic to insulating) occurs simultaneously at U_c. Right panel: results for antiferromagnetic order. Already for $U_c=1$ eV, the Co^{4+} moment is large (the Co^{3+} moment is zero by symmetry) whereas the gap is just beginning to open.

$U < U_c = 3$ eV, the moments on the two inequivalent Co sites are nearly equal and similar to LDA values (which is the $U \rightarrow 0$ limit). Above U_c, disproportionation into $S = 1/2$ Co^{4+} and $S = 0$ Co^{3+} ions is nearly complete at $U = 3.5$ eV and is accompanied by a metal-insulator (Mott-like) transition from conducting to insulating. The gap increases linearly at the rate $dE_g/dU = 0.6$ for $U > 3.5$ eV. For the (insulating) $U = 5$ eV case, nonmagnetic Co^{3+} states lie at the bottom of the 1.3 eV wide gap, with the occupied Co^{4+} e_g' states 1–2 eV lower. The spin-half "hole" on the Co^{4+} ion occupies the a_g orbital as expected.

In our choice of (small) supercell, this CD is necessarily accompanied by charge order, resulting in a honeycomb lattice of spin half ions. In a crystal there would be three distinct choices of the ordered sublattice (corresponding to the three possible sites for Co^{3+}). Of course, even at a rational concentration such as $x = 1/3$, CD may occur without necessarily being accompanied by charge ordering when thermal and quantum fluctuations are accounted for. Regarding the disproportionation, we note that, based on the Mullikan charge decomposition in the FPLO method, the charges on the "Co^{3+}" and "Co^{4+}" ions differ by only 0.25–0.3 electrons. This small value reflects the well-known result that the formal charge designation, while being very informative of the magnetic state and indispensable for physical understanding, does not represent actual charge accurately.

The analogous calculation can be carried out allowing AFM order of the Co^{4+} ions, and the results are shown in the right panel of Fig. 6. A Co^{4+} moment grows (disproportionation) immediately as U is increased from zero. The gap opens around $U = 1$ eV and increases at the rate $dE_g/dU = 0.4$. Thus for AFM spin order, the critical value is no higher than $U_c = 1$ eV.

At $x = 2/3$, CD will lead to only one Co^{4+} ion in the supercell, so only FM ordering can be considered. The corresponding behavior of the moment and the gap are presented in Fig. 7. The Co moments remain nearly equal but slowly decrease from their LDA value up to $U_c = 3$ eV, whereupon again CD occurs abruptly. The moments are "well formed" by $U = 4$ eV but continue to evolve somewhat beyond that. In this case $dE_g/dU = 0.67$.

Our LDA+U results, showing charge disproportionation for $U_c = 3$ eV (FM) or $U_c = 1$ eV (AFM) are very different from earlier reports where little change was obtained even for larger values of U when symmetry breaking by disproportionation was not allowed.[64] This difference serves as an alert that LDA+U results can be sensitive to what degrees of freedom are allowed.

It is far from obvious that charge disproportionation and gap opening should occur simultaneously with LDA+U, although physically the phenomena are expected to be closely related. The evolution of the Co^{3+} and Co^{4+} $3d$ states with U in the critical region is shown in Fig. 8. In the FM case, the system evolves from a half metallic configuration, still visible for $U = 3$ eV, and gap opening occurs just when the minority a_g band containing 2/3 hole per Co ion splits off from the valence band. At the point of separation, the a_g states split into an unoccupied narrow band containing one hole for each of the two Co^{4+} ions, and an occupied (and also narrow) band on the Co^{3+} ion. This disproportionation can be identi-
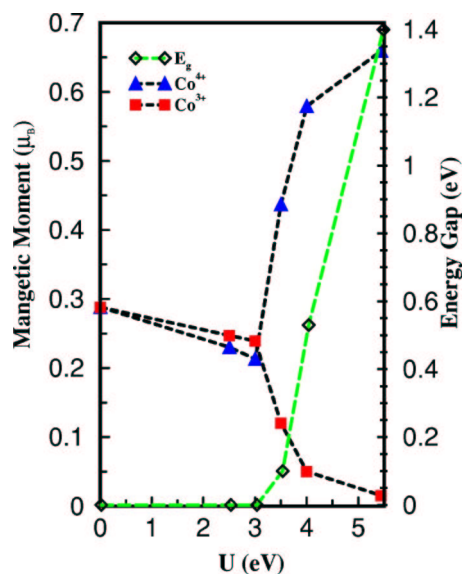

FIG. 7. Effect of the intra-atomic repulsion U on the magnetic moment (left axis) and energy gap (right axis) of the Co1 and Co2 ions in the supercell for $x = 2/3$. Changes in the magnetic moments, indicating disproportionation to formal charge states Co^{3+} and Co^{4+}, begins at $U_c = 3$ eV just as in the corresponding $x = 1/3$ case. Note that applying small but increasing U decreases the moment somewhat until disproportionation occurs. The opening of the gap (half metallic to insulating) occurs simultaneously at U_c.

fied from the strong change in the *occupied* states around -0.6 to -0.3 eV. Thus while disproportionation in principle could occur before the gap opens, it does not do so here.

When symmetry is broken according to the AFM ordered (and disproportionated) superlattice shown in Fig. 2, the critical value of U is 1 eV or less. This "ease" in gap opening is no doubt encouraged by the narrow bandwidth of the unoccupied a_g band. A spin-up Co^{4+} ion is surrounded by three spin-down Co^{4+} ions and three Co^{3+} ions, neither of which have a_g states of the same spin direction at the same energy. The surviving bandwidth reflects the effective coupling between a_g states on second-neighbor Co ions. For this AFM ordered phase, the DOS of Fig. 8 indicates also little or no disproportionation before the gap begins to open.

Exchange coupling. The Coulomb repulsion parameter U has not been calculated for these cobaltates, but several estimates for other cobaltates put U at 5 eV or above.[42,45,49] On the other hand, Chainani *et al.* fit cluster calculation results to x ray photoemission data on samples showing both charge states, and found that U in the 3–5.5 eV range work equally well.[66] This range is rather lower than what has been generally supposed, thus the appropriate value of U is quite uncertain. Here we concentrate on $U = 5.4$ eV results, but our calculated behavior is not sensitive to variation of U in this range. In this CD regime (also charge ordered, due to the constraint of the supercell), AFM ordering gives 1.2 mRy/Co lower energy than does FM order. In terms of nearest-neighbor coupling on the resulting honeycomb lattice, the FM-AFM energy difference corresponds to $J = 11$ meV. Referring to the paramagnetic bandwidth identified above, the corresponding superexchange constant would
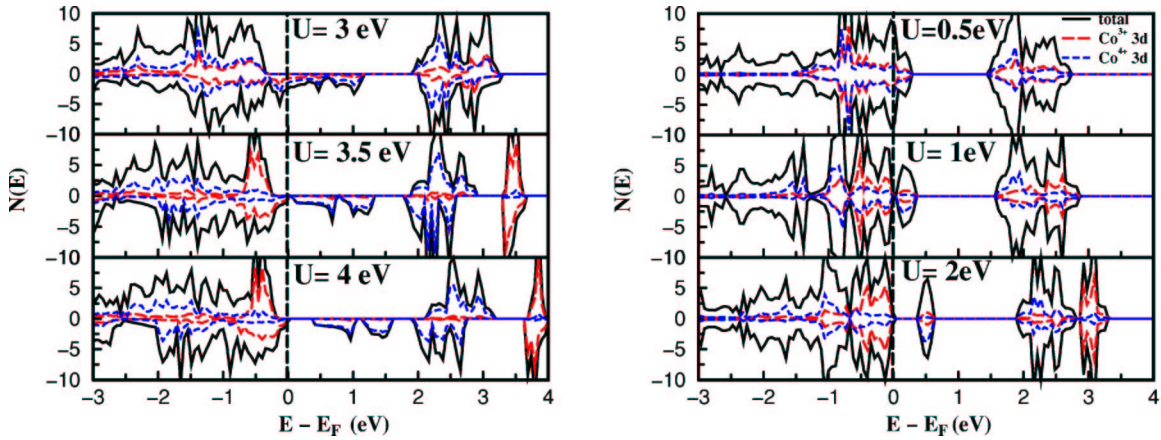
FIG. 8. Evolution of the Co^{3+} and $Co^{4+}3d$ states as charge disproportionation occurs, for $x=1/3$ and FM spin order (left panel) and AFM spin order (right panel). Note that the evolution in the FM case is from a half metallic FM.

be $4t^2/U \sim 20$ meV. Again, we note that the a_g DOS differs greatly from the single band picture that was used to obtain this value of $t=0.16$ eV.

V. DISCUSSION OF INTERACTION STRENGTH

Our calculations indicate that, as long as $U \gtrsim 3$ eV as is generally thought, at both $x=1/3$ and $x=2/3$ there is a strong tendency to disproportionate, with one result being a Co^{4+} ion with a local moment. Disproportionation into an AFM honeycomb lattice occurs already by $U_c=1$ eV in our mean field treatment. At least in the presence of charge order in a honeycomb arrangement, there is an AFM nearest neighbor exchange coupling $J \approx 11$ meV. The Néel state is known to be the ground state of the AFM Heisenberg honeycomb lattice. These charge ordering tendencies may be expected to be strongly opposed by thermal and quantum fluctuations that are expected for low coordination and small spins in 2D layers. To date, disproportionation and charge ordering have only been reported for $x=1/2$.[31]

In addition to producing local magnetic moments, charge disproportionation might be expected to introduce coupling to the lattice. Since the radii of Co^{2+} and Co^{3+} differ by 15% (0.74 Å versus 0.63 Å), disproportionation into those charge states would be expected to couple strongly to local oxygen modes. In octahedral coordination, however, the Co^{4+} ion radius is almost indistinguishable from that of the Co^{3+} ion,[66] so there may be little evidence in the lattice behavior even if Co^{3+}-Co^{4+} charge disproportionation occurs.

In spite of the prevalent theoretical presumption that correlation effects may be playing an essential role in the superconductivity of this cobaltate system, the data seem to be suggesting otherwise. In the $x>0.5$ regime, indeed local moments are evident in thermodynamic and transport data, spin fluctuations have been observed by neutron scattering, and the linear specific heat coefficients are large, $\gamma = 48-56$ mJ/mol K^2. Comparing this value to our calculated band value $\gamma_\circ = 10 \pm 2$ mJ/mol K^2 leads to a factor of five enhancement due to dynamic correlation effects. Magnetic ordering around $x \sim 0.75$ also attests to substantial correlation effects. Our finding of disproportionation for $U > 3$ eV

(in mean field) is consistent with the experimental information and a correlated electron picture.

In the superconducting regime $x \approx 0.3$, the emerging picture is quite the opposite. The specific heat coefficient is ordinary, with the reported values[4,5] clustering around $\gamma = 12-13$ mJ/mol K^2 indistinguishable from the band value $\gamma_\circ \approx 13$ mJ/mol K^2. In addition, there is no local moment (Curie-Weiss) contribution to the susceptibility, and other evidence of enhanced properties is lacking (magnetic field dependence of the resistivity is small, for example). In short, evidence of substantial correlation effects due to the anticipated strong on-site Coulomb repulsion U is difficult to find for $x < 0.5$. Moreover, as discussed in the Introduction, the $x=0$ endpoint is not a Mott insulator, but rather a nonmagnetic metal.[24]

It is essential to begin to reconcile the microscopic model with observations. There are several indications that the simple single band picture is oversimplified, one of the most prominent being that there is no evidence that the a_g state is significantly different in energy from the e'_g states, i.e. the t_{2g} degeneracy is still essentially in place. Due to the form of dispersion in the CoO_2 layer, it is still the case that holes doped into the band insulator $NaCoO_2$ go into the a_g band, making it viable to use a single band model in the small $1-x$ regime with a rather robust value of U, with a value of $U \approx 3$ eV possibly being sufficient to account for correlated electron behavior ($W \approx 1.5$ eV).

The $x < 0.5$ regime seems to require reanalysis. It is quite plausible, based both on the LDA band structure and the observed properties, that for $x < 0.5$, the system crosses over into a three-band regime where the full t_{2g} complex of states comes into play. The multiband nature tends to mitigate correlated behavior in at least two ways. First, doped carriers that go into a multiband complex may simply find a smaller "phase space" for approaching or entering the Mott-Hubbard insulating phase, as the carriers have more degrees of freedom. Not completely separate, perhaps, is the extensive study of Gunnarsson, Koch, and Martin[68,69] and Koch, Gunnarsson, and Martin,[70] that strongly suggests that in a multiband system of N bands, the effective repulsion strength becomes $U^{eff} = U/\sqrt{N}$. For these cobaltates with carriers in the

t_{2g} bands, $N=3$, and $U_c \lesssim 3$ eV would become $U_c^{\text{eff}} \rightarrow 3$ eV$/\sqrt{3} \sim W$, and correlation effects diminish considerably. Second, screening will increase as hole doping occurs from the band insulator $x=1$, reducing—perhaps strongly—the intra-atomic repulsion U to a value near W.

VI. SUMMARY

In this paper we have begun an analysis, coupled with close attention to the observed behavior, of the strength of correlation effects in this cobaltate system that superconducts when hydrated. In this initial work, we have used the mean field LDA+U method to evaluate the effects of Hubbard-like interactions in NxCO, and find charge disproportionation and a Mott insulating state for Coulomb repulsion $U=3$ eV or less, for both $x=1/3$ and $x=2/3$, when fluctuations are neglected. Ferromagnetic tendencies for small U evolve to nearest-neighbor antiferromagnetic coupling $J \approx 11$ meV for $U \sim 5$ eV, at least if charge disproportionation occurs. The only insulating phase reported so far has been at $x=1/2$, with strong evidence[31] that it is due to charge disproportionation and charge order (and probably magnetic order).

The $x=1/3$ LDA FS has been described, following the presumption (based on the observation of at most moderately correlated behavior) that 2D fluctuations will restore the paramagnetic metallic state. There are strong indications however that strong interactions, clearly evident for $x>1/2$, have become muted in the regime where superconductivity appears. On the one hand, the electronic structure and FS indicate that multiband effects must be considered in this regime, which in itself will decrease the effective repulsion U. Independently, U will be decreased by screening as the system becomes increasingly metallic. On the experimental side, the behavior of both the magnetic susceptibility and the linear specific heat coefficient point to a lack of "enhanced" behavior for $x \approx 0.3$.

ACKNOWLEDGMENTS

[1] I. Terasaki, Y. Sasago, and K. Uchinokura, Phys. Rev. B **56**, R12685 (1997).

[2] K. Takada, H. Sakurai, E. Takayama-Muromachi, F. Izumi, R. A. Dilanian, and T. Sasaki, Nature (London) **422**, 53 (2003).

[3] H. Sakurai, K. Takada, S. Yoshii, T. Sasaki, K. Kindo, and E. Takayama-Muromachi, Phys. Rev. B **68**, 132507 (2003).

[4] B. Lorenz, J. Cmaidalka, R. L. Meng, and C. W. Chu, Phys. Rev. B **68**, 132504 (2003).

[5] B. G. Euland, P. Schiffer, R. E. Schaak, M. L. Foo, V. L. Miller, and R. J. Cava, Physica C **402**, 27 (2004).

[6] G. Cao, C. Feng, Y. Xu, W. Lu, J. Shen, M. Fang, and Z. Xu, J. Phys.: Condens. Matter **15**, L519 (2003).

[7] T. Waki, C. Michioka, M. Kato, K. Yoshimura, K. Takada, H. Sakurai, E. Takayama-Muromachi, and T. Sasaki, cond-mat/0306036 (unpublished).

[8] F. C. Chou, J. H. Cho, P. A. Lee, E. T. Abel, K. Matan, and Y. S. Lee, Phys. Rev. Lett. **92**, 157004 (2004).

[9] R. Jin, B. C. Sales, P. Khalifah, and D. Mandrus, Phys. Rev. Lett. **91**, 217001 (2003).

[10] Y. Wang, N. S. Rogado, R. J. Cava, and N. P. Ong, Nature (London) **423**, 425 (2003).

[11] R. E. Schaak, T. Klimczuk, M. L. Foo, and R. J. Cava, Nature (London) **424**, 527 (2003).

[12] Y. Ono, R. Ishikawa, Y. Miyazaki, Y. Ishii, Y. Morlii, and T. Kajitani, J. Solid State Chem. **166**, 177 (2002).

[13] J. W. Lynn, Q. Huang, C. M. Brown, V. L. Miller, M. L. Foo, R. E. Schaak, C. Y. Jones, E. A. Mackey, and R. J. Cava, Phys. Rev. B **68**, 214516 (2003).

[14] J. D. Jorgensen, M. Avdeev, D. G. Hinks, J. C. Burely, and S. Short, Phys. Rev. B **68**, 214517 (2003).

[15] R. Siegel, J. Hirschinger, D. Carlier, M. Ménétrier, and C. Delmas, Solid State Nucl. Magn. Reson. **23**, 243 (2003).

[16] Y. Takahashi, Y. Gotoh, and J. Akimoto, J. Solid State Chem. (to be published).

[17] C. Delmas, J. J. Braconnier, C. Fouassier, and P. Hagenmueller, Solid State Ionics **3/4**, 165 (1981).

[18] Y. G. Shi, H. C. Yu, C. J. Nie, and J. Q. Li, cond-mat/0401052 (unpublished).

[19] J. van Elp, J. L. Wieland, H. Eskes, P. Kuiper, G. A. Sawatzky, F. M. F. de Groot, and T. S. Turner, Phys. Rev. B **44**, 6090 (1991).

[20] M. T. Czyzyk, P. Potze, and G. A. Sawatzky, Phys. Rev. B **46**, 3729 (1992).

[21] G. C. Amatucci, J. M. Tarascon, and L. C. Klein, J. Electrochem. Soc. **143**, 1114 (1996).

[22] L. Seguin, G. Amatucci, M. Anne, Y. Chabre, P. Strobel, J. M. Tarascon, and G. Vaughan, J. Power Sources **81–82**, 604 (1999).

[23] J. M. Tarascon, G. Vaughan, Y. Chabre, L. Seguin, M. Anne, P. Strobel, and G. Amatucci, J. Solid State Chem. **147**, 410 (1999).

[24] J. M. Tarascon (private communication).

[25] C. J. Milne, D. N. Argyriou, A. Chemseddine, N. Aliouane, J. Viera, and D. Alber, cond-mat/0401273 (unpublished).

[26] A. Lerf and R. Schöllhorn, Inorg. Chem. **16**, 2950 (1977).

[27] D. C. Johnston and B. W. Keelan, Solid State Commun. **52**, 631 (1984).

[28] D. C. Johnston, Mater. Res. Bull. **17**, 13 (1982).

[29] D. C. Johnston and S. P. Frysinger, Phys. Rev. B **30**, 980 (1984).

[30] D. C. Johnston, J. Less-Common Met. **84**, 327 (1982).

[31] M. L. Foo, Y. Wang, S. Watauchi, H. W. Zandbergen, T. He, R. J. Cava, and N. P. Ong, Phys. Rev. Lett. **92**, 247001 (2004).

[32] M. L. Foo, R. E. Schaak, V. L. Miller, T. Kliimczuk, N. S. Rogado, Y. Wang, G. C. Lau, C. Craley, H. W. Zandbergen, N. P. Ong, and R. J. Cava, Solid State Commun. **127**, 33 (2003).

[33] R. Motohashi, R. Ueda, E. Naujalis, T. Tojo, I. Terasaki, T. Atake, M. Karppinen, and H. Yamauchi, Phys. Rev. B **67**, 064406 (2003).

[34] J. Sugiuyama, H. Itahara, J. H. Brewer, E. J. Ansaldo, T. Motohashi, M. Karppinen, and H. Yamauchi, Phys. Rev. B **67**, 214420 (2003).

[35] J. Sugiuyama, J. H. Brewer, E. J. Ansaldo, H. Itahara, T. Tani, M. Mikami, Y. Mori, T. Sasaki, S. Hébert, and A. Maignan, Phys. Rev. Lett. **92**, 017602 (2004).

[36] A. T. Boothroyd, R. Coldea, D. A. Tennant, D. Prabhakaran, L. M. Helme and C. D. Frost, Phys. Rev. Lett. **92**, 197201 (2004).

[37] Y. Ando, N. Miyamoto, K. Segawa, T. Kawata, and I. Terasaki, Phys. Rev. B **60**, 10580 (1999).

[38] The unusual susceptibility observed by Sakurai *et al.* (Ref. 3) with $d\chi/dT$ positive above 130 K, was interpreted to include a Curie-Weiss term that would imply a Co moment of the order of 0.01 μ_B.

[39] Y. Kobayashi, M. Yokoi, and M. Sato, J. Phys. Soc. Jpn. **72**, 2453 (2003).

[40] P. W. Anderson, Mater. Res. Bull. **8**, 153 (1973).

[41] B. Bernu, P. Lecheminant, C. Lhuiller, and L. Pierre, Phys. Rev. B **50**, 10048 (1994).

[42] D. J. Singh, Phys. Rev. B **61**, 13397 (2000).

[43] D. J. Singh, Phys. Rev. B **68**, 020503 (2003).

[44] R. Koretsune and M. Ogata, Phys. Rev. Lett. **89**, 116401 (2002).

[45] M. Ogata, J. Phys. Soc. Jpn. **72**, 1839 (2003).

[46] B. Kumar and B. S. Shastry, Phys. Rev. B **68**, 104508 (2003).

[47] R. Moessner and S. L. Sondhi, Prog. Theor. Phys. Suppl. **145**, 37 (2002).

[48] Q.-H. Wang, D.-H. Lee, and P. A. Lee, cond-mat/0304377 (unpublished).

[49] A. Tanaka and X. Hu, Phys. Rev. Lett. **91**, 257006 (2003).

[50] C. Honerkamp, Phys. Rev. B **68**, 104510 (2003).

[51] G. Baskaran, Phys. Rev. Lett. **91**, 097003 (2003); cond-mat/0306569 (unpublished).

[52] W. Koshibae and S. Maekawa, Phys. Rev. Lett. **91**, 257003 (2003).

[53] Von M. Jansen and F. Hoppe, Z. Anorg. Allg. Chem. **408**, 104

[53] (1974).

[54] P. Blaha, K. Schwarz, G. K. H. Madsen, D. Kvasnicka, and J. Luitz, *Wien2k, An Augmented Plane Wave and Local Orbitals Program for Calculating Crystal Properties* (Karlheinz Schwarz, Technical Universität Wien, Wien 2001), ISBN 3-950/031-1-2.

[55] P. Novak, F. Boucher, P. Gressier, P. Blaha, and K. Schwarz, Phys. Rev. B **63**, 235114 (2001).

[56] A. B. Shick, A. I. Liechtenstein, and W. E. Pickett, Phys. Rev. B **60**, 10763 (1999).

[57] E. Sjöstedt, L. Nordström, and D. J. Singh, Solid State Commun. **114**, 15 (2000).

[58] K. Koepernik and H. Eschrig, Phys. Rev. B **59**, 1743 (1999).

[59] H. Eschrig, *Optimized LCAO Method and the Electronic Structure of Extended Systems* (Springer, Berlin, 1989).

[60] V. I. Anisimov, I. V. Solovyev, M. A. Korotin, M. T. Czyzyk, and G. A. Sawatzky, Phys. Rev. B **48**, 16929 (1993).

[61] M. T. Czyzyk and G. A. Sawatzky, Phys. Rev. B **49**, 14211 (1994).

[62] H. Rosner, S.-L. Dreschler, F. Fuchs, A. Handstein, A. Wälte, and K.-H. Müller, Braz. J. Phys. **33**, 718 (2003).

[63] M. D. Johannes and D. J. Singh, Phys. Rev. B (to be published).

[64] Earlier LDA+U calculations did not allow ordering: L.-J. Zou, J.-L. Wang, and Z. Zeng, cond-mat/0307560 (unpublished).

[65] A. Chainani *et al.*, cond-mat/0312293 (unpublished). These authors use the term "charge order" which appears to us to simply designate charge disproportionation rather than actual (short- or long-range) order.

[66] http://www.webelements.com/webelements/elements/-print/Co/radii.html

[67] W. E. Pickett, J. M. An, R. Rosner, and S. Y. Savrasov, Physica C **387**, 117 (2003).

[68] O. Gunnarsson, E. Koch, and R. M. Martin, Phys. Rev. B **54**, R11026 (1996).

[69] O. Gunnarsson, E. Koch, and R. M. Martin, Phys. Rev. B **56**, 1146 (1997).

[70] E. Koch, O. Gunnarsson, and R. M. Martin, Comput. Phys. Commun. **127**, 137 (2000).